Alternative Medicine & Chiropractic Open Access Journal
ISSN: 2642-0171

Research Article *Volume 2; Issue 3*

Assessment of Physical, Thermal and Spectral Properties of the Consciousness Energy Healing Treated Magnesium Gluconate

Mahendra KT[1] and Snehasis J[2]*

[1]Trivedi Global, Inc, Henderson, USA

[2]Trivedi Science Research Laboratory Pvt Ltd, Thane (W), India

***Corresponding author:** Snehasis Jana, Trivedi Science Research Laboratory Pvt Ltd, Thane (W), Maharashtra, India, Tel: +91-022-25811234; Email: publication@trivedieffect.com

Received Date: July 16, 2019; **Published Date:** August 16, 2019

Abstract

Magnesium plays a crucial role in the functioning of cells and in the regulation of tRNA and rRNA structures of the human body. Thus, magnesium gluconate (Mg-gluconate) is given as nutraceutical supplements as a source of magnesium. The objective of the study was to analyse the impact of the Trivedi Effect®- Consciousness Energy Healing Treatment on the physical, thermal, and spectral properties of Mg-gluconate. Thus, the experiment involves dividing the Mg-gluconate sample into two parts. One part of the samples was treated remotely by the famous Biofield Energy Healer, Mr. Mahendra Kumar Trivedi with the Biofield Energy Healing Treatment termed as a treated sample and the untreated part was termed as a control sample. Both the samples were analyzed using sophisticated analytical techniques.

The powder XRD relative peak intensities and crystallite sizes of the treated Mg-gluconate showed significant alterations in the range of -13.28% to 41.71% and -57.12% to 100.12%, respectively, along with a decrease of 6.33% in the average crystallite size as compared to the control sample. Further, the particle size values of the treated sample were found to be significantly increased by 2.80% (d_{10}), 28.25% (d_{50}), 25.56% (d_{90}), and 24.59% {D(4,3)}; while the surface area was decreased by 8.87% as compared to the control sample.

The vaporisation temperature of the treated sample was decreased by 6.43% compared to the control sample. However, the latent heat of vaporization and fusion of the treated sample were significantly decreased by 9.58% and 5.98%, respectively. Besides, the TGA/DTG data showed 0.21% decrease in the total weight loss of the treated sample compared with the control sample. The maximum thermal degradation temperature values for two peaks of the treated sample also reduced by 2.34% and 0.97%, compared to the control sample. The study indicated that the Consciousness Energy Healing Treatment might be helpful in producing a new polymorphic form of Mg-gluconate that may also possess a better appearance, flowability, storage, and stability profile compared to the control sample. Thus, the Biofield Energy Treatment may be useful in the designing of better quality nutraceutical/pharmaceutical formulations for the improved responses against the magnesium deficiency and prevention and treatment of several diseases.

Keywords: Magnesium gluconate; The Trivedi Effect®; Energy of Consciousness Healing Treatment; Particle size; DSC; TGA.

Citation: Mahendra KT and Snehasis J. Assessment of Physical, Thermal and Spectral Properties of the Consciousness Energy Healing Treated Magnesium Gluconate. Alt Med Chiropractic OA J 2019, 2(3): 180022.

Abbreviations: Mg: Magnesium; RNA: Ribonucleic Acid; AMP: Adenosine Monophosphate; tRNA: Transfer Ribonucleic Acid; ADP: Nicotinamide Adenine Dinucleotide Phosphate; ATP: Adenosine Triphosphate; DNA: Deoxyribonucleic Acid.

Introduction

Magnesium (Mg) is one among the most abundant and important mineral in the human body due to its wide application in various metabolic processes. It helps in the normal functioning of cells, nerves, muscles, bones, etc. and thereby plays a crucial role in the body functions [1]. Mg^{2+} is a major intracellular ion, which plays an important role in the structural regulation of tRNA and rRNA also takes place with the help of intracellular magnesium ions [2]. Moreover, the enzymes using AMP, ADP, or ATP as substrates ion and plays a role in the processing of RNA and DNA also use magnesium ions as their cofactor [3-5].

Although a balanced diet is sufficient in fulfilling the normal requirement of magnesium in the body, but some clinical situations may cause more loss of this ion from the body, such as severe diarrhea/vomiting, stomach/intestinal absorption problems, diabetes, certain drugs, and alcoholism, etc. [6,7]. The magnesium deficiency symptoms include muscle weakness, fatigue, nausea, loss of appetite, etc. and it required the replenishment of magnesium in the body with the help of supplements [8]. Magnesium gluconate ($MgC_{12}H_{22}O_{14}$), which is the magnesium salt of gluconic acid, is used as a magnesium supplement and it shows the maximum bioavailability than the other magnesium supplements available in the market [9, 10].

Apart from treating the deficiency symptoms, it is also used in the prevention and treatment of several other diseases such as septic shock, diabetes mellitus, immunological disorders, allergies, inflammatory diseases, and other chronic infections [11-12]. Mg-gluconate can also be used as laxative and antacid that helps in treating the heartburn and indigestion by reacting with the stomach acid and thereby increases the gastric pH [9]. Some studies also reported its role in blocking the free radical flow in the treatment of ischemia/reperfusion injury due to oxidative stress [13]. Besides, the other uses of Mg-gluconate supplements include the regulation of blood pressure, prevention of cardiovascular disorders and in the treatment of mild to moderate persistent asthma [14]. The bioavailability profile of several drugs may also get affected by the Trivedi Effect®-Energy of Consciousness Healing Treatment, which has been known in recent days for its impact on altering the solubility as well as the bioavailability of various pharmaceutical/nutraceutical compounds [15-17]. It uses the Biofield Energy Healing and a Biofield Healing practitioner transmitted the life force energy (Biofield Energy), which is a type of electromagnetic field around the human body [18]. There are several Biofield (Putative Energy Fields) based Energy Healing Therapies that are used nowadays against various disease conditions [19,20]. Also, the Biofield Energy Healers has the ability to harness the energy from the "Universal Energy Field" and can transmit it into any living or non-living object(s). Further, the process of receiving the Biofield Energy Treatment by the objects and responding into a useful way is known as the Biofield Energy Healing Treatment.

The National Center of Complementary and Integrative Health has recognized and accepted Biofield based Energy Healing therapies as a Complementary and Alternative Medicine health care approach in addition to other medicines, therapies, and practices such as chiropractic/osteopathic manipulation, yoga, Tai Chi, Qi Gong, homeopathy, essential oils, massage, meditation, progressive relaxation, acupressure, acupuncture, hypnotherapy, rolfing Ayurvedic medicine, naturopathy, cranial sacral therapy, traditional Chinese herbs and medicines, Reiki, aromatherapy, applied prayer, etc. [19]. The impact of the Trivedi Effect® was observed in various fields such as, organic compounds pharmaceuticals nutraceuticals material science microbiology biotechnology and agricultural [21-33]. It is well known that the physicochemical and thermal properties of any compound play an important role in their performance [34,35]. Thus, the objective of this study was to assess the impact of the Trivedi Effect® on the physicochemical, thermal and spectroscopic properties of Mg-gluconate. Such an assessment was done by using several sofisticated analytical techniques.

Materials and Methods

Chemicals and Reagents

The test sample magnesium gluconate was purchased from Tokyo Chemical Industry Co., Ltd., Japan, and other chemicals were purchased in India.

Consciousness Energy Healing Treatment Strategies

The test compound Mg-gluconate was divided into two parts. Among the two parts, one portion was denoted as control sample that did not receive the Biofield Energy Treatment. Besides, the other part of Mg-gluconate was considered as Biofield Energy Treated sample, which received the Energy of Consciousness Healing Treatment

by the famous Biofield Energy Healer, Mr. Mahendra Kumar Trivedi (USA), remotely for 3 minutes through his Unique Energy Transmission process under the standard laboratory conditions. On the other hand, the control Mg-gluconate was treated with a "sham" healer under the same laboratory conditions, who have no awareness about the Biofield Energy. Consequently, both the Mg-gluconate samples were kept in similar sealed conditions and further characterized by using sophisticated techniques.

Characterization

The powder X-ray diffraction (PXRD) analysis of Mg-gluconate powder sample was performed with the help of PANalytical X'Pert3 Pro [26,36]. The average size of crystallites was calculated using the Scherrer's formula (1)

$$G = k\lambda/\beta\cos\theta \qquad (1)$$

Where G = crystallite size in nm, k = equipment constant (0.5), λ = radiation wavelength, β = full-width at half maximum, and θ = Bragg angle [37]. The particle size distribution (PSD) analysis was performed with the help of Malvern Mastersizer 3000, UK instrument using the wet method. Similarly, the differential scanning calorimetry (DSC) analysis of Mg-gluconate was performed with the help of DSC Q200, TA instruments. The thermal gravimetric analysis (TGA) thermograms of Mg-gluconate were performed with the help of TGA Q50 TA instruments.

Ultraviolet-visible spectroscopy (UV-Vis) analysis was carried out using Shimadzu UV-2400PC series, Japan. Fourier transform infrared (FT-IR) spectroscopy of Mg-gluconate was performed on Spectrum ES (Perkin Elmer, USA) FT-IR spectrometer [26,36]. The % change in the above parameters of the Biofield Energy Treated Mg-gluconate was calculated compared to the control sample using the equation 2:

$$\% \text{ Change} = [(\text{Treated} - \text{Control}) / \text{Control}] \times 100. \qquad (2)$$

Results and Discussion

Powder X-ray Diffraction (PXRD) Analysis

The PXRD diffractograms (Figure 1) showed sharp peaks that represent the crystalline nature of Mg-gluconate samples. The data revealed that the crystallite sizes of the Biofield Energy Treated Mg-gluconate were significantly altered ranging from -57.12% to 100.12% compared with the control sample. Likewise, the average crystallite size of the Biofield Energy Treated sample was observed as 41.58µm, which was significantly decreased by 6.33% in comparison to the control sample (44.39µm). Besides, the highest peak intensity (100%) in the PXRD diffractogram of both the samples was observed at 5.0° (Table 1). The relative intensity of the peaks of Biofield Energy Treated sample was significantly altered ranging from -13.28% to 41.71% in comparison to the control sample, thereby suggested the significant alterations in the crystal properties of the Biofield Energy Treated sample after treatment.

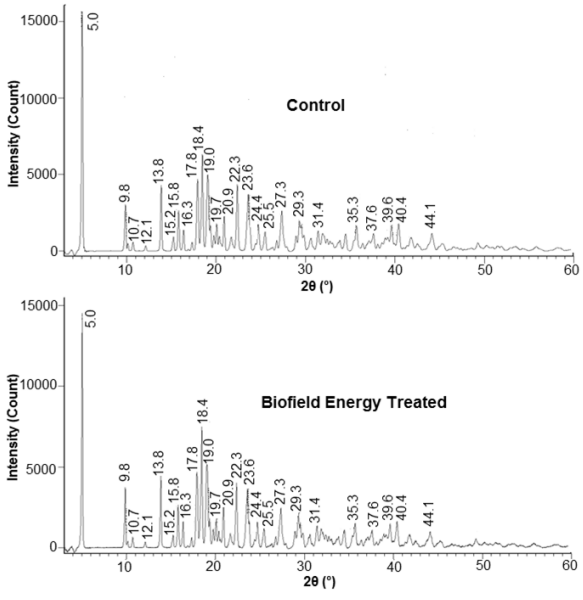

Figure 1: PXRD diffractograms of the control and treated Mg-gluconate.

Entry No.	Bragg angle (°2θ)	Relative Peak Intensity (%)			Crystallite size (G, nm)		
		Control	Treated	% Change*	Control	Treated	% Change*
1	5.0	100.00	100.00	0.00	49.22	57.36	16.54
2	9.8	17.91	25.38	41.71	49.36	43.18	-12.52
3	10.7	3.76	4.71	25.27	49.39	49.39	0.00
4	12.1	2.15	2.50	16.28	24.71	49.45	100.12
5	13.8	27.83	30.95	11.21	38.52	38.52	0.00
6	15.2	6.02	5.60	-6.98	43.41	57.82	33.20
7	15.8	16.64	18.85	13.28	38.61	34.74	-10.02
8	16.3	8.67	11.34	30.80	38.63	38.63	0.00
9	17.8	28.47	31.78	11.63	43.55	31.66	-27.30
10	18.4	40.51	50.97	25.82	38.74	38.74	0.00
11	19.0	32.36	33.10	2.29	49.59	49.59	0.00
12	19.7	6.64	8.11	22.14	43.67	38.81	-11.13
13	20.9	14.52	17.53	20.73	31.81	29.16	-8.33
14	22.3	28.39	28.23	-0.56	38.98	43.86	12.52
15	23.6	23.19	24.91	7.42	43.96	43.96	0.00
16	24.4	3.19	3.36	5.33	25.15	44.02	75.03
17	25.5	7.60	7.86	3.42	58.77	25.20	-57.12
18	27.3	17.13	17.06	-0.41	44.28	50.61	14.30
19	29.3	12.84	14.55	13.32	71.09	39.53	-44.39
20	31.4	8.53	9.35	9.61	44.70	39.73	-11.12
21	35.3	4.14	4.66	12.56	36.12	30.10	-16.67
22	37.6	7.37	7.27	-1.36	36.36	25.97	-28.58
23	39.6	10.99	9.53	-13.28	91.40	40.66	-55.51
24	40.4	11.65	11.41	-2.06	33.34	52.42	57.23
25	44.1	7.56	6.98	-7.67	46.44	46.44	0.00

Table 1**:** PXRD data for the control and treated Mg-gluconate.

*denotes the percentage change in the relative intensity and crystallite size of the treated sample compared to the control sample.

Denotes the percentage change in the relative intensity and crystallite size of the treated sample compared to the control sample. The literature reported that the relative intensity across each plane of the crystalline compound may vary based on the crystal morphology [38]. Also, the altered relative intensity of the characteristic peaks suggested that the crystallinity of Biofield Energy Treated sample might be altered compared to the control sample. Thus, it is presumed that the Biofield Energy might induce the formation of more symmetrical crystalline long range pattern after getting absorbed by the treated Mg-gluconate that caused the increase in the intensity of peaks. Hence, the energy transferred *via* the Biofield Energy Healing Treatment probably altered the size and shape of molecules, thereby altering the crystallinity and crystallite size of the treated sample as compared to the control sample. Moreover, some studies mentioned the changes in XRD pattern as the sign of polymorphic transitions [39,40] which may further affect the solubility, dissolution, and bioavailability parameters of the drug [41]. Hence, the PXRD study revealed that Biofield Energy Healing Treatment might produce a new polymorphic form of zinc chloride, which could have improved the bioavailability profile as compared with the control sample.

Particle Size Analysis (PSA)

The particle size and surface area of both the samples were calculated and presented in Table 2. The particle size distribution data revealed the significant increase in the particle size values of the Biofield Energy Treated Mg-gluconate at d_{10}, d_{50}, d_{90}, and D(4,3) and it was observed to be increased by 2.80%, 28.25%, 25.56%, and 24.59%, respectively as compared with the control sample. However, the specific surface area (SSA) of Biofield Energy Treated Mg-gluconate (197.2 m^2/Kg) was significantly decreased by 8.87% with respect to the control sample (216.4 m^2/Kg), which might be due to the increase in the particle size of the Biofield Energy Treated sample after the treatment (Figure 1).

Test Item	d_{10} (µm)	d_{50} (µm)	d_{90} (µm)	D(4,3) (µm)	SSA(m^2/Kg)
Control	10.7	43.9	180.0	72.8	216.4
Biofield Energy Treated	11.0	56.3	226.0	90.7	197.2
Percent change (%)	2.80	28.25	25.56	24.59	-8.87

Table 2: Particle size distribution of the control and treated Mg-gluconate.
d_{10}, d_{50}, and d_{90}: particle diameter corresponding to 10%, 50%, and 90% of the cumulative distribution, SSA: the specific surface area, D(4,3): the average mass-volume diameter.

The reason behind this decrease in the surface area credited to the increased particle size of the treated sample after the Biofield Energy Treatment [42]. According to some previous studies, the particle size of the compound may upsurge along with an increase in thermal energy. Thus, it is presumed that the Biofield Energy Treatment might act in this way and reduced the thermodynamically driving force, which affected the decrease in nucleus densities and thereby enhanced the particle size [43, 44]. This increased particle size of the Biofield Energy Treated sample might be useful in enhancing the appearance, shape, and flowability of the compound [45, 46].

Differential Scanning Calorimetry (DSC) Analysis

The DSC data revealed the presence of two endothermic peaks in the thermograms of both the Mg-gluconate samples (Figure 2). Among these, the first peak (minor) of thermogram might be considered to be generated as a result of the evaporation of the water from the sample, as the Mg-gluconate is usually occurring in the hydrate form. The comparative analysis revealed that the Biofield Energy Treated sample showed a significant alteration in this vaporization temperature as well as the latent heat of vaporization in comparison to the control sample.

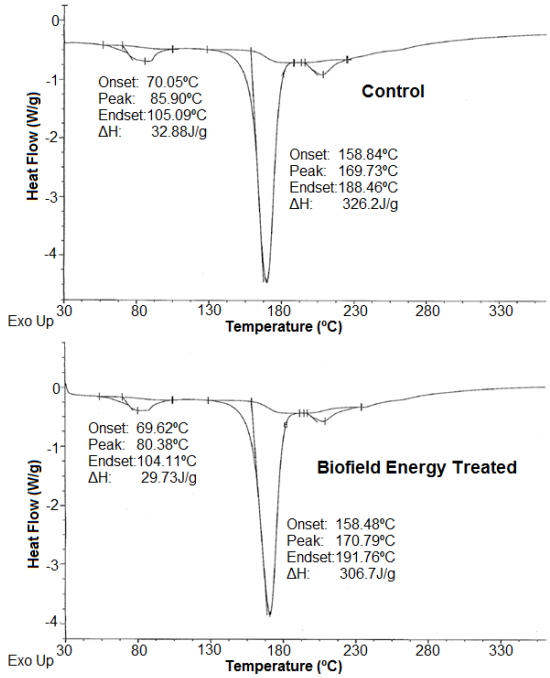

Figure 2: DSC thermograms of the control and treated Mg-gluconate.

The vaporisation temperature in the Biofield Energy Treated sample was observed at 80.38°C, which was decreased by 6.43% as compared to the control sample (85.90°C). Similarly, the latent heat of vaporization of the Biofield Energy Treated sample was found as 29.73J/g that is 9.58% less as compared to the control sample (32.88J/g). Besides, the second sharp endothermic peak (major) was considered to appear as a result of the melting of Mg-gluconate (Figure 2).

The Biofield Energy Treated Mg-gluconate showed almost similar melting point (170.79°C) as that of the control sample (169.73°C), but the latent heat of fusion (ΔH_{fusion}) was significantly decreased by 5.98% in the Biofield Energy Treated Mg-gluconate compared to the control sample (Table 3). The study suggested that the latent heat energy (ΔH) requirement of the Biofield Energy Treated Mg-gluconate undergo the process of melting, differs from the control sample. Thus, it might be indicating some alterations in the intermolecular forces after the Biofield Energy Treatment, which may be responsible for such change in ΔH.

Peak	Description	Melting Point (°C)	ΔH (J/g)
Peak 1 (Minor)	Control sample	85.90	32.88
	Biofield Treated sample	80.38	29.73
	% Change	-6.43	-9.58
Peak 2 (Major)	Control sample	169.73	326.20
	Biofield Treated sample	170.79	306.70
	% Change	0.62	-5.98

Table 3: The latent heat of fusion (J/G) and melting point (°C) values of the control and treated Mg-gluconate.

ΔH: Latent heat of vaporization/fusion

Thermal Gravimetric Analysis (TGA)/ Differential Thermogravimetric Analysis (DTG)

The TGA/DTG analysis was done for determining the thermal stability of the samples, with the help of thermograms of both the samples (Figures 3 and 4). Apart from that, the TGA and DTG data for both the samples are given in (Tables 4 and 5). The thermograms of both the samples showed three-step thermal degradation, in which, the weight loss of the Biofield Energy Treated sample at the 1st step was found to be significantly increased by 66.20%, compared to the control sample. On the other hand, the treated Mg-gluconate showed decreased weight losses by 5.24% and 5.30% in the 2nd and 3rd steps of thermal degradation as compared to the control sample.

However, the total weight loss of the Biofield Energy Treated sample showed a slight decrease of 0.21% compared with the control sample (Table 4). In addition, the degradation temperatures corresponding to this three-step degradation of the Biofield Energy Treated sample also showed variations as compared to the control sample. The 1st step of degradation in the treated sample was observed at 164.50°C as compared to the control sample (155.24°C). Similarly, the degradation temperature of 2nd step of the Biofield Energy Treated sample also showed an increase and was observed at 260.69°C as compared to the control sample (257.13°C).

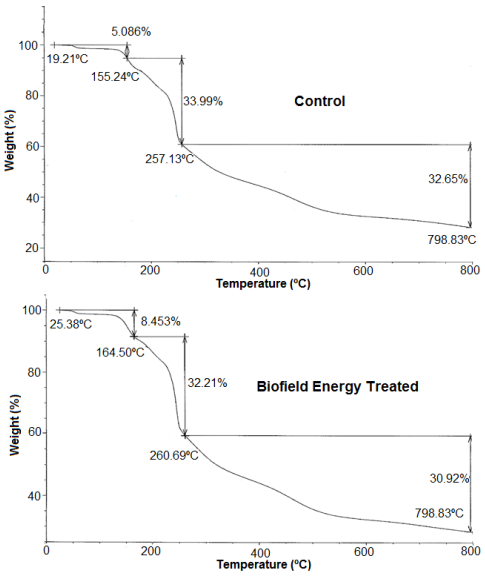

Figure 3: TGA thermograms of the control and treated Mg-gluconate.

Step	Temperature (°C)		Weight loss %		% Change
	Control	Treated	Control	Treated	
1st step of degradation	155.24	164.50	5.086	8.453	66.20
2nd step of degradation	257.13	260.69	33.99	32.21	-5.24
3rd step of degradation	798.83	798.83	32.65	30.92	-5.30
Total weight loss	-	-	71.73	71.58	-0.21

Table 4: Thermal degradation steps of the control and treated Mg-gluconate.

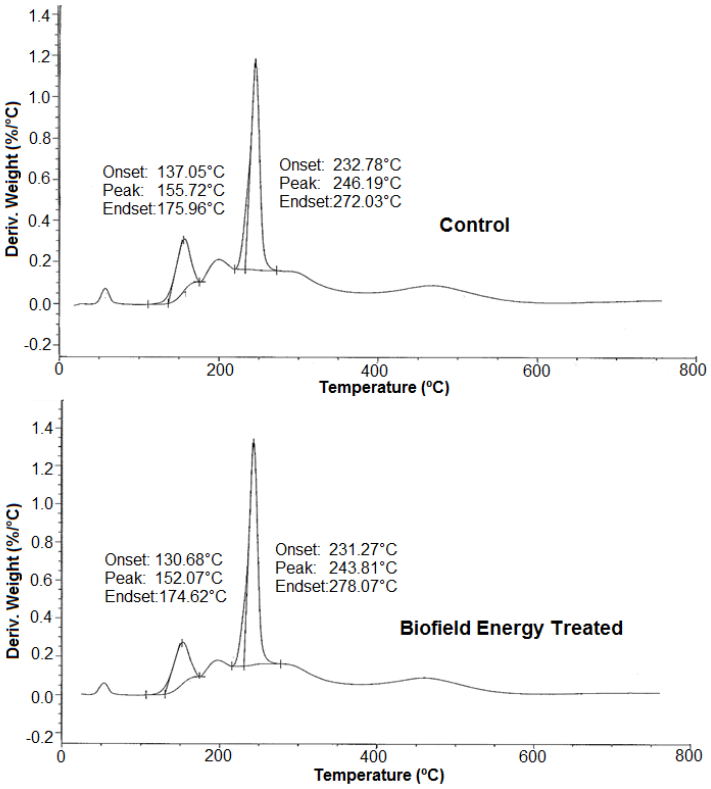

Figure 4: DTG thermograms of the control and treated Mg-gluconate.

Step	1st Peak		% Change	2nd Peak		% Change
	Control	Treated		Control	Treated	
Onset Temperature	137.05	130.68	-4.65	232.78	231.27	-0.65
Peak Temperature	155.72	152.07	-2.34	246.19	243.81	-0.97
Endset Temperature	175.96	174.62	-0.76	272.03	278.07	2.22

Table 5: The DTG thermal degradation steps of the control and treated Mg-gluconate.
T_{max} = maximum thermal degradation temperature.

The DTG thermograms of the control and Biofield Energy Treated samples (Figure 4) exhibited two peaks. The analysis revealed the alterations in the onset, peak and endset temperatures of both the peaks of the Biofield Energy Treated sample as compared to the control. The onset temperature of the 1st peak of the Biofield Energy Treated sample was observed at 130.68°C, which was decreased by 4.65% than the control sample (137.05°C).

Similarly, the maximum thermal degradation temperature (T_{max}) and the endset temperature of the 1st peak of the Biofield Energy Treated sample were also decreased by 2.34% and 0.76%, respectively, as compared to the control sample (Table 5). Consequently, the 2nd peak of the DTG thermogram of the treated Mg-gluconate sample also showed alterations in the onset, peak and endset temperatures as -0.65%, -0.97%, and 2.22%, respectively, compared to the control sample (Table 5). Overall, the TGA/DTG analysis showed the alteration in the thermal stability of the Biofield Energy Treated Mg-gluconate, which might be due to the alteration in particle size of the Biofield Energy Treated sample as compared to the control sample.

Ultraviolet-visible Spectroscopy (UV-Vis) Analysis

The UV-visible spectra of both, the control and Biofield Energy Treated Mg-gluconate samples are presented in Figure 5. The UV-vis spectra of the treated Mg-gluconate sample showed the maximum absorbance (λ_{max}) at 202 nm, which is similar as that of the control sample; thus, there was no significant alteration between the control and Biofield Energy Treated sample in terms of the absorbance maxima. It concluded that there might not be any significant change induced by the Biofield Energy Treatment in the electronic transitions between the highest occupied molecular orbital (HOMO) and lowest unoccupied molecular orbital (LUMO) [47].

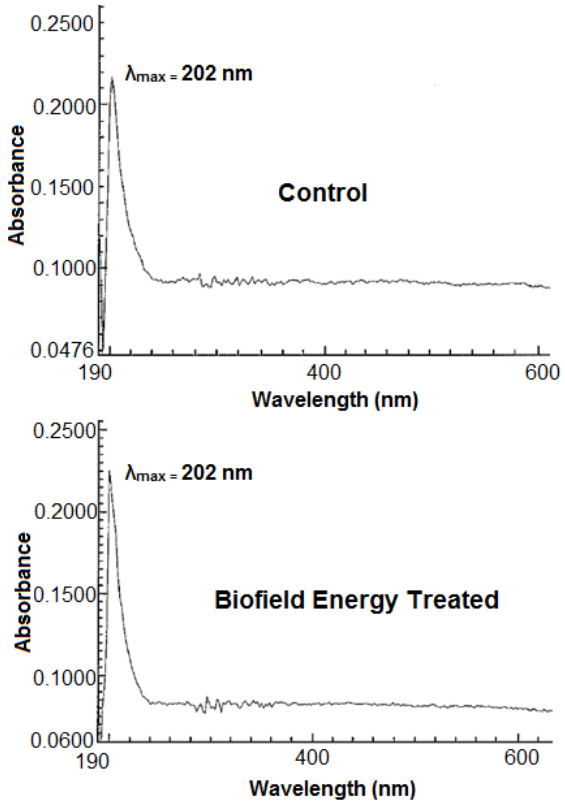

Figure 5: UV-vis spectra of the control and treated Mg-gluconate.

Fourier Transform Infrared (FT-IR) Spectroscopy

The FT-IR spectra of both the control and Biofield Energy Treated Mg-gluconate are shown in Figure 6, which involves the visible stretching and bending peaks in the functional group as well as the fingerprint region [48]. The spectra of the control and Biofield Energy Treated samples showed broad peaks in the functional group area near 3396 and 3398 cm^{-1}, respectively that may be assigned to the O-H stretching present in the primary and secondary alcohol as well as the water molecules of Mg-gluconate hydrate.

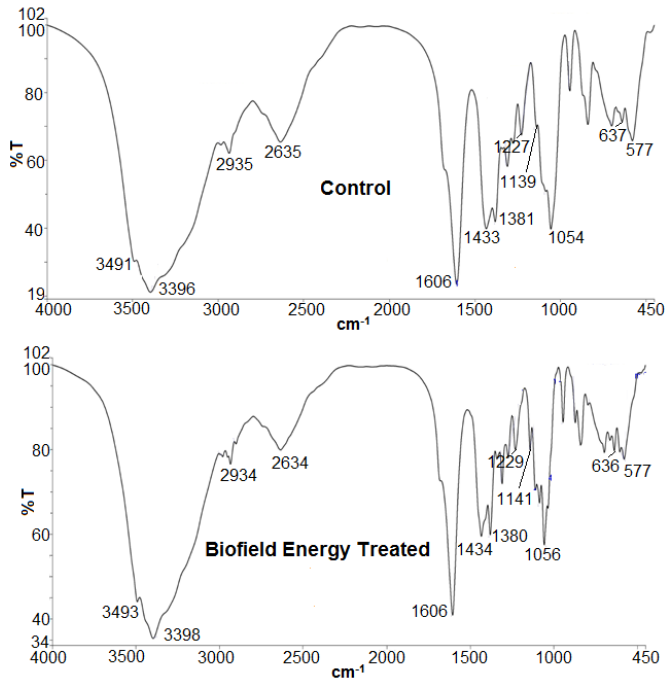

Figure 6: FT-IR spectra of the control and treated Mg-gluconate.

This water peak may appear as a result of the stretching vibrations of hydroxyl groups from the water present in Mg-gluconate hydrate. Apart from that, there may also be the stretching vibrations of the primary and secondary hydroxyl groups of the gluconate, which may get merged in the intensive broad band of the water molecules [36]. Also, the spectra involves the deformation vibration peaks (in plane δ(OH) and out-of-plane γ(OH)) of the hydroxyl groups, which were observed at 1433 cm^{-1} and 637 cm^{-1} and 577 cm^{-1}, respectively in the spectrum of the control sample, whereas, at 1434 cm^{-1} and 636 cm^{-1} and 577 cm^{-1}, respectively in the spectrum of Biofield Energy Treated sample.

Similarly, the spectra showed C-H stretching at 2935 and 2934 cm^{-1} for the control and Biofield Energy Treated samples, respectively. Moreover, the peaks regarding the asymmetric and symmetric vibrations of C=O of the carboxylate anion were observed in the form of intensive peaks at 1606 and 1381 cm^{-1} in the spectrum of a control sample; whereas, at 1606 and 1380 cm^{-1} in the spectrum of the Biofield Energy Treated sample. Later on, the C-O stretching vibration peaks regarding the secondary alcoholwere observed at 1227 cm^{-1} and 1139 cm^{-1} in the spectrum of the control sample, whereas at 1229 cm^{-1} and 1141 cm^{-1} in the spectrum of the Biofield Energy Treated sample. Similarly, the peak regarding C-O stretching vibrations of the primary alcohol group was observed at 1054 and 1056 cm^{-1} in the spectra of the control and Biofield Energy Treated sample, respectively. The overall FT-IR analysis showed no significant alteration in the Biofield Energy Treated sample and the control samples in terms of the frequency of the characteristic peaks. Thus, it might be concluded that the chemical structure of the Mg-gluconate hydrate remained the same in both the Biofield Energy Treated and control samples.

Conclusion

The overall study concluded the impact of the Trivedi Effect® - Consciousness Energy Healing Treatment on the physicochemical and thermal properties of Mg-gluconate. The powder XRD relative peak intensities and crystallite sizes of the treated Mg-gluconate showed significant alterations in the range of -13.28% to 41.71% and -57.12% to 100.12%, respectively, along with a decrease of 6.33% in the average crystallite size as compared to the control sample. Such changes in the crystallite size as well as the relative intensities of characteristic peaks of the Biofield Energy Treated sample indicated that there was some alteration in the morphology, crystallinity, and the polymorphic form of the Mg-gluconate hydrate after the Biofield Energy Treatment. The particle size values of the treated sample were found to be significantly increased

by 2.80% (d_{10}), 28.25% (d_{50}), 25.56% (d_{90}), and 24.59% {D(4,3)}; while the surface area was observed to be decreased by 8.87% as compared to the control sample.

The altered particle size and surface area of the Biofield Energy Treated Mg-gluconate may help in improving the shape, appearance, and flowability of the compound. The vaporisation temperature of the treated sample was decreased by 6.43% compared to the control sample. However, the $\Delta H_{vaporisation}$ and ΔH_{fusion} of the treated sample were significantly decreased by 9.58% and 5.98%, respectively. Besides, the TGA/DTG data showed 0.21% decrease in the total weight loss of the treated sample compared to the control sample. The T_{max} values for two peaks of the treated sample also reduced by 2.34% and 0.97%, compared to the control sample. Hence, the overall study concluded that the Energy of Consciousness Healing Treatment might be helpful in altering the polymorphic form, crystallinity and particle size of Mg-gluconate that may provide it a better appearance, flowability, and bioavailability profile with altered thermal stability. Therefore, the Energy of Consciousness Healing Treatment would be very useful in the designing of better formulation for the treatment of various disorders, such as cancer, septic shock, arrhythmias, inflammatory diseases, allergies, diabetes mellitus, immunological disorders, asthma, gestational hypertension, etc.

Acknowledgements

The authors are grateful to GVK Biosciences Pvt. Ltd., Trivedi Science, Trivedi Global, Inc., and Trivedi Master Wellness for their assistance and support during this work.

References

1. Guerrera MP, Volpe SL, Mao JJ (2009) Therapeutic Uses of Magnesium. Am Fam Physician 80(2): 157-162.

2. Takaya J, Higashino H, Kobayashi Y (2004) Intracellular magnesium and insulin resistance. Magnes Res 17(2): 126-136.

3. Ronconi L, Sadler PJ (2008) Applications of heteronuclear NMR spectroscopy in biological and medicinal inorganic chem. Coordn Chem Rev 252(21): 2239-2277.

4. Swaminathan R (2003) Magnesium metabolism and its disorders. Clin Biochem Rev 24(2): 47-66.

5. Trivedi MK, Tallapragada RM, Branton A, Trivedi D, Nayak G, et al. (2015) Potential impact of biofield treatment on atomic and physical characteristics of magnesium. Vitam Miner 3: 129.

6. Alaimo K, McDowell MA, Briefel RR, Bischof AM, Caughman CR, et al. (1994) Dietary intake of vitamins, minerals, and fiber of person ages 2 months and over in the United States: Third National Health and Nutrition Examination Survey, Phase 1, 1988-91. Adv Data (258): 1-28.

7. LaValle JB (2006) Hidden disruptions in metabolic syndrome: Drug-induced nutrient depletion as a pathway to accelerated pathophysiology of metabolic syndrome. Altern Ther Health Med 12(2): 26-31.

8. Feinstein A (1996) Prevention's healing with vitamins: The most effective vitamin and mineral treatments for everyday health problems and serious disease-- From allergies and arthritis to water retention and wrinkles. Prevention Magazine Health Books, Rodale.

9. Gropper SS, Smith JL, Groff JL (2005) Magnesium. In: Advanced Nutrition and Human Metabolism (4th ed) Wadsworth Publishing, Belmont, Calif.

10. Coudray C, Rambeau M, Feillet-Coudray C, Gueux E, Tressol JC, et al. (2005) Study of magnesium bioavailability from ten organic and inorganic Mg salts in Mg-depleted rats using a stable isotope approach. Magnes Res 18(4): 215-223.

11. Fleming TE, Mansmann Jr HC (1999) Methods and compositions for the prevention and treatment of immunological disorders, inflammatory diseases and infections. United States Patent 5939394, 1-11.

12. Fleming TE, Mansmann Jr HC (1999) Methods and compositions for the prevention and treatment of diabetes mellitus. United States Patent 5871769, 1-10.

13. Weglicki WB (2000) Intravenous magnesium gluconate for treatment of conditions caused by excessive oxidative stress due to free radical distribution. United States Patent 6100297, 1-6.

14. Barbagallo M, Dominguez LJ, Galioto A, Ferlisi A, Cani C, et al. (2003) Role of magnesium in insulin action, diabetes and cardiometabolic syndrome X. Mol Aspects Med 24(1-3): 39-52.

15. Trivedi MK, Mohan TRR (2016) Biofield Energy Signals, Energy Transmission and Neutrinos, Amer J Modern Phy 5: 172-176.

16. Trivedi MK, Branton A, Trivedi D, Nayak G, Balmer AJ, et al. (2017) Study of the energy of consciousness healing treatment on physical, structural, thermal, and behavioral properties of zinc chloride. Modern Chem 5(2): 19-28.

17. Trivedi MK, Branton A, Trivedi D, Nayak G, Balmer AJ, et al. (2017) Evaluation of physicochemical, spectral, thermal and behavioral properties of the biofield energy healing treated sodium selenate. Sci J Chem 5(2): 12-22.

18. Rubik B, Muehsam D, Hammerschlag R, Jain S (2015) Biofield Science and Healing: History, Terminology, and Concepts. Glob Adv Health Med4: 8-14.

19. Koithan M (2009) Introducing complementary and alternative therapies. J Nurse Pract 5(1): 18-20.

20. Movaffaghi Z, Farsi M (2009) Biofield therapies: Biophysical basis and biological regulations? Complement Ther Clin Pr 15(1): 35-37.

21. Trivedi MK, Branton A, Trivedi D, Nayak G, Bairwa K, et al. (2015) Physical, thermal, and spectroscopic characterization of biofield energy treated methyl-2-naphthyl ether. J Environ Anal Chem 2: 162.

22. Trivedi MK, Branton A, Trivedi D, Nayak G, Bairwa K, et al. (2015) Impact of biofield treatment on spectroscopic and physicochemical properties of p-nitroaniline. Insights Analyl Electrochem1: 1-8.

23. Trivedi MK, Patil S, Shettigar H, Singh R, Jana S (2015) An impact of biofield treatment on spectroscopic characterization of pharmaceutical compounds. Mod Chem Appl 3: 159.

24. Trivedi MK, Branton A, Trivedi D, Nayak G, Bairwa K, et al. (2015) Spectroscopic characterization of disulfiram and nicotinic acid after biofield treatment. J Anal Bioanal Tech 6: 265.

25. Trivedi MK, Branton A, Trivedi D, Nayak G, Plikerd WD, et al. (2017) A systematic study of the biofield energy healing treatment on physicochemical, thermal, structural, and behavioral properties of magnesium gluconate. International Journal of Bioorganic Chemistry 2(3): 135-145.

26. Trivedi MK, Branton A, Trivedi D, Nayak G, Plikerd WD, et al. (2017) A systematic study of the biofield energy healing treatment on physicochemical, thermal, structural, and behavioral properties of iron sulphate. Int J Bio Chem. 2: 135-145.

27. Trivedi MK, Tallapragada RM, Branton A, Trivedi D, Nayak G, et al. (2015) The Potential impact of biofield energy treatment on the atomic and physical properties of antimony tin oxide nanopowder. American J Optics and Photonics 3(6): 123-128.

28. Trivedi MK, Tallapragada RM, Branton A, Trivedi D, Nayak G, et al. (2015) Characterization of physical and structural properties of aluminum carbide powder: Impact of biofield treatment. J Aeronaut Aerospace Eng 4: 142.

29. Trivedi MK, Patil S, Shettigar H, Gangwar M, Jana S (2015) Antimicrobial Sensitivity Pattern of *Pseudomonas fluorescens* after Biofield Treatment. J Infect Dis Ther 3: 222.

30. Trivedi MK, Branton A, Trivedi D, Nayak G, Mondal SC, et al. (2015) Evaluation of plant growth regulator, immunity and DNA fingerprinting of biofield energy treated mustard seeds (*Brassica juncea*). Agriculture, Forestry and Fisheries 4(6): 269-274.

31. Trivedi MK, Patil S, Shettigar H, Gangwar M, Jana S (2015) *In vitro* evaluation of biofield treatment on cancer biomarkers involved in endometrial and prostate cancer cell lines. J Cancer Sci Ther 7: 253-257.

32. Trivedi MK, Branton A, Trivedi D, Nayak G, Gangwar M, et al. (2015) Evaluation of vegetative growth parameters in biofield treated bottle gourd (*Lagenaria siceraria*) and okra (*Abelmoschus esculentus*), Int J Nutrition and Food Sci 4(6): 688-694.

33. Trivedi MK, Branton A, Trivedi D, Nayak G, Mondal SC, et al. (2015) Impact of biofield energy treatment on soil fertility. Earth Sciences 4(6): 275-279.

34. Storey RA, Ymen I (2011) Solid state characterization of Pharmaceuticals, Wiley-Blackwell, UK.

35. Gupta KR, Askarkar SS, Joshi RR, Padole YF (2015) Solid state properties: Preparation and characterization. Der Pharmacia Sinica 6(4): 45-64.

36. Trivedi MK, Branton A, Trivedi D, Nayak G, Lee AC, et al. (2017) A comprehensive analytical evaluation of

the Trivedi Effect® - Energy of Consciousness Healing Treatment on the physical, structural, and thermal properties of zinc chloride. American Journal of Applied Chemistry 5(1): 7-18.

37. Langford JI, Wilson AJC (1978) Scherrer after sixty years: A survey and some new results in the determination of crystallite size. J Appl Cryst 11: 102-113.

38. Inoue M, Hirasawa I (2013) The relationship between crystal morphology and XRD peak intensity on $CaSO_4.2H_2O$. J Crystal Growth 380: 169-175.

39. Raza K, Kumar P, Ratan S, Malik R, Arora S (2014) Polymorphism: The phenomenon affecting the performance of drugs. SOJ Pharm Pharm Sci 1(2): 10.

40. Thiruvengadam E, Vellaisamy G (2014) Polymorphism in pharmaceutical ingredients a review. World Journal of Pharmacy and Pharmaceutical Sciences 3: 621-633.

41. Blagden N, de Matas M, Gavan PT, York P (2007) Crystal engineering of active pharmaceutical ingredients to improve solubility and dissolution rates. Adv Drug Deliv Rev 59: 617-630.

42. Sun J, Wang F, Sui Y, She Z, Zhai W, et al. (2012) Effect of particle size on solubility, dissolution rate, and oral bioavailability: Evaluation using coenzyme Q10 as naked nanocrystals. Int J Nanomedicine 7: 5733-5744.

43. Katayama M (1956) The crystal structure of an unstable form of chloroacetamide. Acta Crystallogr 9: 986-991.

44. Rashidi AM, Amadeh A (2009) The effect of saccharin addition and bath temperature on the grain size of nanocrystalline nickel coatings. Surf Coat Technol 204(3): 353-358.

45. Buckton G, Beezer AE (1992) The relationship between particle size and solubility. Int J Pharmaceutics 82(3): R7-R10.

46. Mosharrof M, Nystrom C (1995) The effect of particle size and shape on the surface specific dissolution rate of microsized practically insoluble drugs. Int J Pharm 122(1): 35-47.

47. Hesse M, Meier H, Zeeh B (1997) Spectroscopic methods in organic chemistry, Georg Thieme Verlag Stuttgart, New York.

48. Stuart BH (2004) Infrared spectroscopy: Fundamentals and applications in Analytical Techniques in the Sciences. John Wiley & Sons Ltd., Chichester, UK.